energy&fuels

Article

pubs.acs.org/EF

Solid-Phase Extraction Fractionation To Extend the Characterization of Naphthenic Acids in Crude Oil by Electrospray Ionization Fourier Transform Ion Cyclotron Resonance Mass Spectrometry

Steven M. Rowland,[†] Winston K. Robbins,[‡] Yuri E. Corilo,[‡] Alan G. Marshall,[†,§] and Ryan P. Rodgers*[,†,‡,§]

[†]Department of Chemistry and Biochemistry, Florida State University, 95 Chieftain Way, Tallahassee, Florida 32306, United States

[‡]Future Fuels Institute, and [§]Ion Cyclotron Resonance Program, National High Magnetic Field Laboratory, Florida State University, 1800 East Paul Dirac Drive, Tallahassee, Florida 32310, United States

ABSTRACT: Naphthenic (NAP) acids have been previously characterized by negative electrospray ionization (ESI) Fourier transform ion cyclotron resonance mass spectrometry (FT-ICR MS), both directly and from acid extracts. Here, we show that collective characterization of NAP acids with negative-ion ESI, both with and without prior extraction, results in a loss of signal from high mass acids because of ion suppression by low mass acids. We have developed an extraction to simultaneously isolate and fractionate NAP acids into distinct molecular weight ranges, thereby grouping acids into fractions with similar ionization efficiency. A NAP acid fraction was isolated (all acids isolated collectively in one fraction) and compared to NAP acid isolation by molecular weight. Characterization of acid molecular weight fractions extended the observed upper mass limit from ∼850 Da for the collectively isolated acids to ∼1450 Da for the acids isolated by molecular weight range, thereby approximately doubling the observed mass range for NAP acids. Plots of double bond equivalents (DBE = number of rings plus double bonds to carbon) versus carbon number span both higher carbon number and higher DBE values than are accessed by collective acid characterization. The high mass resolving power and mass accuracy of FT-ICR MS are essential for identification and resolution of acidic species across a wide mass range.

INTRODUCTION

Venezuela, Canada, and Russia are among the countries that possess the largest proven petroleum reserves,[1] with the largest oil reserves located in the Americas.[2] Furthermore, most deepwater discoveries in areas such as west Africa, South America, Canada, and the Gulf of Mexico will be from reservoirs with ideal conditions for microbial degradation.[2] As the world oil supply shifts from light sweet crude oils to heavy biodegraded oil, the need for characterization of polar crude oil species has greatly increased. Crude oils typically consist of ∼85−90% hydrocarbons and ∼10−15% polar and moderately polar compounds.[3] However, heavy oils are often enriched in metals (e.g., iron, vanadium, and nickel) and more polar heteroatom (sulfur, nitrogen, and oxygen) containing compounds.[3] Heavy crude oils often exhibit extensive biodegradation, resulting in highly oxygenated acidic species. Naphthenic (NAP) acids are among the most abundant oxygen-containing components and are conventionally defined as carboxylic acids that may contain multiple saturated rings. However, the term has recently evolved to encompass all petroleum carboxylic acids (e.g., aliphatic, alicyclic, and aromatic).[4] Organic acids have been implicated in causing corrosion in oil refineries, production deposits, sludge formation, emulsion stabilization, and contamination of oil sands process-affected water.[4−11] Therefore, complete and accurate characterization of NAP acid samples is imperative.

NAP acids have been isolated from their parent crudes by various techniques. Column chromatography can separate crude oil into fractions based on different polarities.[12−16] However, polarity-based fractionation techniques, such as saturates, aromatics, resins, and asphaltenes (SARA) separations, yield a fraction that is enriched in not only NAP acids but also other polar crude oil compounds. Liquid−liquid extractions with caustic water/ethanol mixtures are more discriminatory and predominately isolate acidic species[17−20] but tend to isolate low molecular weight/water-soluble acids. Ionic liquids have also been employed to isolate acids from crude oil, but accomplish only 67% removal of NAP acids.[21] During the past decade, solid-phase extractions (SPEs) have become the most widely used techniques for acid isolation from crude oils based on a wide range of SPE phases of which weak- and strong-anion-exchange phases are the most popular.[7,22−25]

Various analytical techniques have been used for NAP acid characterization. Estimates of total acid number (TAN) use both a non-aqueous potentiometric titration and Fourier transform mid-infrared spectroscopy with attenuated total reflection to quantify the number of acidic groups.[26,27] High-performance liquid chromatography (HPLC), both normal and reversed-phase, can isolate and separate NAP acid fractions, but adequate resolution by HPLC with spectroscopic detection is not achievable for such compositionally complex samples.[28,29] Mass spectral detection coupled with liquid chromatography (LC−MS) can provide the added resolution necessary for NAP acid characterization, but ultrahigh-resolution mass spectrom-

Received: July 3, 2014
Revised: July 24, 2014
Published: August 12, 2014

   dx.doi.org/10.1021/ef5015023 | *Energy Fuels* 2014, 28, 5043−5048

etry is needed to resolve mass spectral peaks for most petroleum-derived samples.[30,31] Gas chromatography in tandem with mass spectrometry (GC−MS) and comprehensive two-dimensional gas chromatography/mass spectrometry) (GC × GC−MS) can characterize esterified[5,18,32] NAP acids, assuming a complete reaction. GC-based methods provide higher chromatographic resolution than LC methods but are limited to volatile compounds (e.g., boiling point < 330 °C),[18,33] precluding analysis of high molecular weight (especially polar) species. It has been reported that high-temperature GC (HTGC) can improve the analysis of less volatile species;[34] however, few instances of HTGC analyses for NAP acids have been reported, perhaps because of thermal decomposition of acids.

Electrospray ionization (ESI) produces negative ions by deprotonation. Because the strongest acids in petroleum are carboxylic acids, ESI is particularly efficient at ionizing NAP acids, requiring no sample pretreatment.[8,23,24,35−39] However, it was recently shown under aqueous electrospray conditions that not all acids ionize with equal ionization efficiency.[40] Here, we show that low molecular weight acids dominate the ESI process and suppress ionization of the higher mass (less efficiently ionized) acids. We demonstrate a technique for the simultaneous isolation of NAP acids and separation into distinct molecular weight ranges. The separation by molecular weight isolates NAP acids into fractions with more similar ionization efficiency, thereby increasing the dynamic range for each fraction and extending the attainable upper mass limit to well above 1 kDa.

EXPERIMENTAL SECTION

Materials. Canadian bitumen was deasphalted with *n*-heptane (mixture of 40:1 *n*-heptane/sample was refluxed for 1 h and allowed to cool overnight). The deasphalted oil was isolated by gravity filtration with Whatman (GE Healthcare Bio-Sciences, Pittsburgh, PA) prepleated 113v (30 μm, 150 mm diameter) filter paper and dried under N_2 for analysis. Dichloromethane (DCM), methanol (MeOH), *n*-heptane, and water (H_2O) were J.T.Baker chemicals (Swedesboro, NJ), HPLC grade, and anhydrous toluene was from Sigma-Aldrich (St. Louis, MO). All solvents were used as received. Sigma-Aldrich formic acid (MS grade, ∼98%) was used for the elution of acidic species. Separations were performed with Agilent Bond Elut NH_2 2 g SPE cartridges, as described in detail below. Sigma-Aldrich ammonium hydroxide (28% in H_2O) was used to aid in deprotonation of acids for ESI.

Separation Scheme. Two separation schemes based on an aminopropyl silica (APS) SPE phase are outlined in Figure 1. Scheme 1 isolates NAP acids collectively in one fraction, whereas scheme 2 isolates NAP acids in six fractions corresponding to different molecular weight ranges. Elution solvent and percent recovery are listed with each fraction name. SPE cartridges were conditioned with approximately 12 mL of DCM prior to separation. Samples were dissolved in 1 mL of DCM and loaded dropwise onto the SPE cartridge. The samples were allowed to equilibrate with the SPE phase for ∼15 min before initiating elution at ∼1 mL/min. Approximately 100 mg of oil was loaded onto the SPE cartridges for APS extraction, whereas approximately 500 mg of oil was loaded onto cartridges for modified APS (MAPS) extraction. Scheme 1 takes advantage of the strong hydrogen-bonding interaction between APS and carboxylic acids. Note that we do not refer to this retention mechanism as ion exchange because the interaction between analyte and stationary phase takes place under non-aqueous conditions, where protonation and deprotonation of the amine and acid functionalities are unlikely. The non-acidic species and moderately acidic species are eluted from the cartridge with DCM and DCM−MeOH, whereas the carboxylic acids elute by a displacement mechanism with the addition of formic acid to the eluent. Our MAPS extraction is shown in scheme 2. The same displacement mechanism is used in MAPS extraction; however, after elution with DCM−MeOH, the mobile phase is switched to a reversed-phase composition (with MeOH and MeOH−H_2O washes). When formic acid (FA) is introduced into the eluent, the acids elute by a reversed-phase mechanism because of the propyl functionality of the APS stationary phase, allowing for the simultaneous extraction and fractionation of NAP acids by hydrophobicity, which, for petroleum, also corresponds to alkylation or number of carbon atoms. Fractions were collected in preweighed glass vials, and solvent was evaporated under a gentle stream of nitrogen. It should be noted that the percent recoveries for CN 1 and CN 2 are slightly different from the percent recoveries for MN 1 and MN 2. We believe that the higher mass on column for MAPS extraction leads to overloading of the non-acidic compounds (some of the species that should report to the MN 2 fraction actually elute in the MN 1 fraction). However, for both experiments, the percent recovery of NAP acids was ∼3.5%, indicating that there was no overloading of NAP acids.

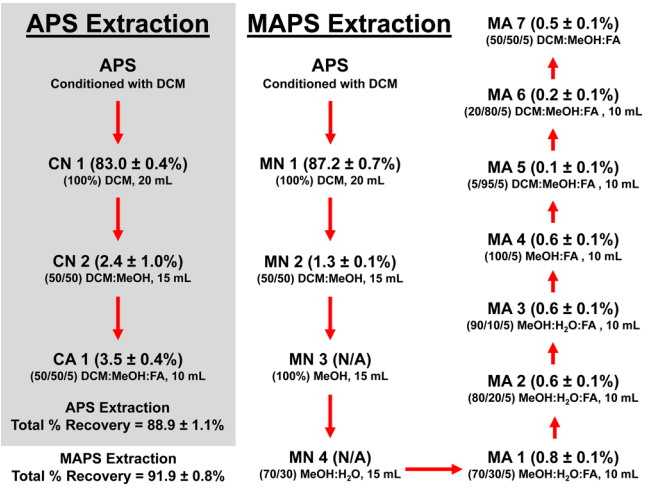

Figure 1. Separation scheme for APS and MAPS NAP acid extractions. The percent recoveries and elution volumes are listed for each fraction as well as total percent recovery for each extraction scheme. The notation N/A is used for fractions for which there was no measurable mass recovery. CN and CA stand for collectively isolated non-acids and collectively isolated acids. MN and MA denote MAPS non-acids and MAPS acids. Error was determined by triplicate analysis.

Sample Preparation for Fourier Transform Ion Cyclotron Resonance Mass Spectrometry (FT-ICR MS). Samples were analyzed at concentrations between 5 and 100 μg/mL. NAP acid fractions were dissolved in toluene to 1 mg/mL and then further diluted with MeOH to the final electrospray concentration. Samples were spiked with NH_4OH in MeOH such that the final ammonia concentration was 0.25%. A syringe pump was used to deliver samples, at a flow rate of 500 nL/min, through a 50 μm inner diameter fused silica micro ESI needle under typical ESI conditions (2.5 kV; heated metal capillary temperature of ∼100 °C).

Mass Analysis. Samples were analyzed with a custom-built passively shielded 9.4 T FT-ICR mass spectrometer equipped with a 22 cm horizontal room-temperature bore.[41] Data acquisition and analysis were performed with a modular ICR data station (Predator).[42] Negative ions were generated at atmospheric pressure and transferred into the mass spectrometer by way of a dual-stage radio frequency (rf) focusing ion funnel.[43] The pressure in funnel 1 was ∼2.7 Torr, and the pressure in funnel 2 was ∼270 mTorr. The capillary voltage was 310 V, and four direct current (DC) voltages were used to apply a voltage gradient across the ion funnel (120, 70, 40, and 10 V). Ions were externally accumulated[44] in an rf-only quadrupole, passed through a mass-resolving rf-only quadrupole, and collisionally cooled with helium (∼3.5 × 10^{-6} Torr) in an rf-only octopole. After cooling, ions were transferred by octopole ion guides to a seven-segment open cylindrical cell with capacitively coupled excitation electrodes.[45,46] A

dx.doi.org/10.1021/ef5015023 | Energy Fuels 2014, 28, 5043−5048

broadband frequency sweep ("chirp") excitation (~70−720 kHz at a sweep rate of 50 Hz/μs and amplitude, V_{p-p}, of 0.67 V) was used to accelerate ions to a cyclotron orbital radius detected as the differential image current between opposed electrodes in the ICR cell. The experimental event sequence was controlled by a Predator data station.[42] Multiple time-domain acquisitions (≥100) were conditionally co-added for each sample,[47] Hanning-apodized, and zero-filled once before fast Fourier transform and magnitude calculation.

Mass Calibration and Data Processing. Mass spectra were externally calibrated with HP mix (Agilent, Santa Clara, CA) standard, and ICR frequencies were converted to m/z based on the quadrupolar trapping potential approximation.[48,49] Peak lists were generated for all peaks with magnitudes greater than 6 standard deviations above the baseline noise. Each mass spectrum was phase-corrected[50] and internally calibrated with a "walking" calibration[47] based on the most abundant homologous alkylation series. Ion masses were then converted to the Kendrick mass scale and sorted into homologous series for each heteroatom class (i.e., ions with the same heteroatom composition ($O_oN_nS_s$), differing only by the degree of alkylation (i.e., number of CH_2 groups).[51] Peak assignments and data visualization were performed with PetroOrg software.[52] Peak assignments were limited to chemical formulas with less than 100 ^{12}C, 200 ^{1}H, 3 ^{14}N, 10 ^{16}O, and 4 ^{32}S atoms.

RESULTS AND DISCUSSION

Characterization of Collectively Isolated NAP Acids. A bitumen sample was deasphalted with *n*-heptane and loaded onto a preconditioned APS SPE cartridge in DCM. The non-carboxylic acid species were eluted in two steps with DCM and DCM/MeOH (50:50, v/v). NAP acids were then eluted with a mixture of DCM/MeOH/FA (50:50:5, v/v/v). All carboxylic acids are thereby collectively isolated from the crude oil in one chromatographic fraction (CA 1). The CA 1 acid fraction was evaporated under dry nitrogen, redissolved in toluene, and electrosprayed in TOL/MeOH (50:50, v/v) with ~0.2% NH_4OH to aid in deprotonation. The resulting mass spectrum (Figure 2) shows a distribution centered at ~425 Da and extending up to ~850 Da, in good agreement with previously reported Canadian bitumen (−) ESI mass spectra.[24,35] The (−) ESI-derived heteroatom class distribution is also shown in Figure 2. Relative abundances of heteroatom classes are typically derived only from the monoisotopic peaks. However, because the relative abundances for ^{13}C isotopologues increase with increasing number of carbon atoms, it is more accurate to sum the relative abundances for all assigned ^{13}C isotopologues.

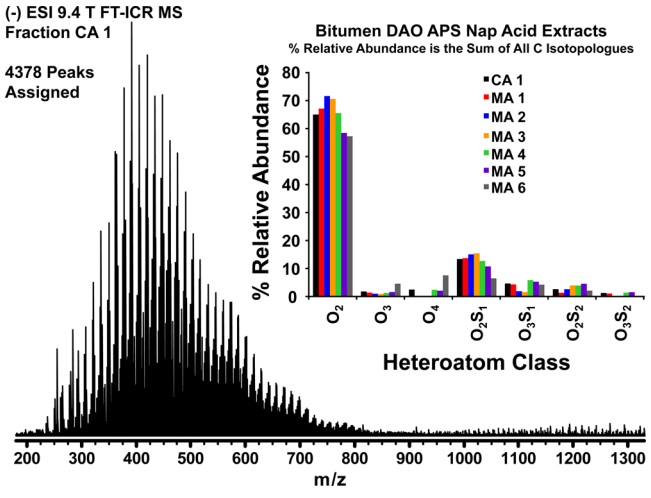

Figure 2. Negative ESI FT-ICR mass spectrum of the collectively isolated acid fraction for APS extraction. (Inset) Heteroatom class distribution for APS and MAPS fractions. Percent relative abundances are calculated for the sum of all detected carbon isotopologues.

All isolated acid fractions consist primarily of O_{2+x} and $O_{2+x}S_y$ compounds, indicating carboxylic acid functionalities. On the basis of previous analyses,[24] the data from the collectively isolated NAP acids (scheme 1) appear not to be limited by mass; however, Figure 3 shows that low-molecular-weight acids dominate the ionization process and suppress the ionization/detection of high-molecular-weight acids, as discussed below.

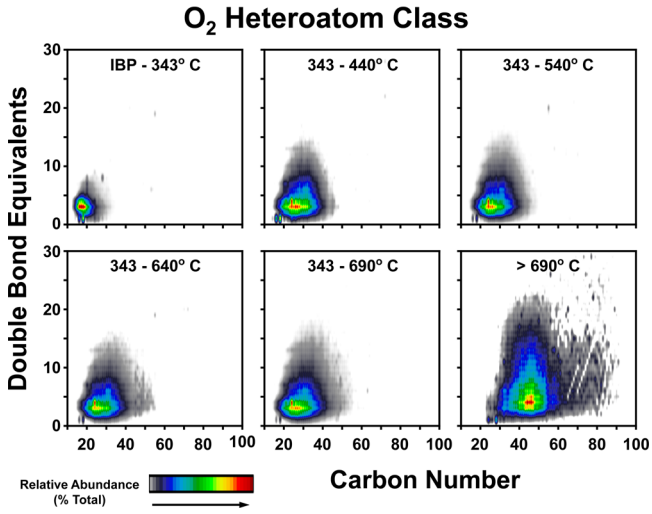

Figure 3. Negative ESI FT-ICR MS-derived isoabundance-contoured plots of DBE versus carbon number for a series of distillation "broad cuts".

Analysis of Distillation "Broad Cuts". A series of distillation boiling point cuts were collected for a Canadian bitumen sample. The lowest boiling point range collected was the initial boiling point (IBP) to 343 °C. The remaining oil was then fractionated in a series of distillations into broad cuts with increasing end temperature. The boiling point ranges along with isoabundance-contoured plots of DBE versus number of carbon atoms are listed in Figure 3. A final sample consisted of the compounds that distill above 690 °C.

According to the Boduszynksi model,[3] each increase in boiling point range should be accompanied by an increase in the number of carbon atoms. Indeed, sequential narrow distillate cuts from similar Canadian bitumen display a systematic increase in carbon number with increasing boiling point.[53] However, the broad cuts shown in Figure 3 do not show a monotonic increase in carbon number. The fraction collected from IBP to 343 °C is centered at carbon number 17, whereas the next boiling range (343−440 °C) is centered at carbon number 26. The increase in carbon number follows the petroleum continuum model as expected. However, the next three boiling point ranges (343−540, 343−640, and 343−690 °C) show little or no change. The residual compounds, with boiling points of >690 °C, show a sharp increase in the carbon number, centered at ~45 carbon atoms. Because the low-molecular-weight NAP acids are present in each fraction, they suppress less ionizable acids of higher carbon number. The increase in carbon number for the most abundant peaks is seen only after low-molecular-weight acids are removed in the final residual fraction.

dx.doi.org/10.1021/ef5015023 | Energy Fuels 2014, 28, 5043−5048

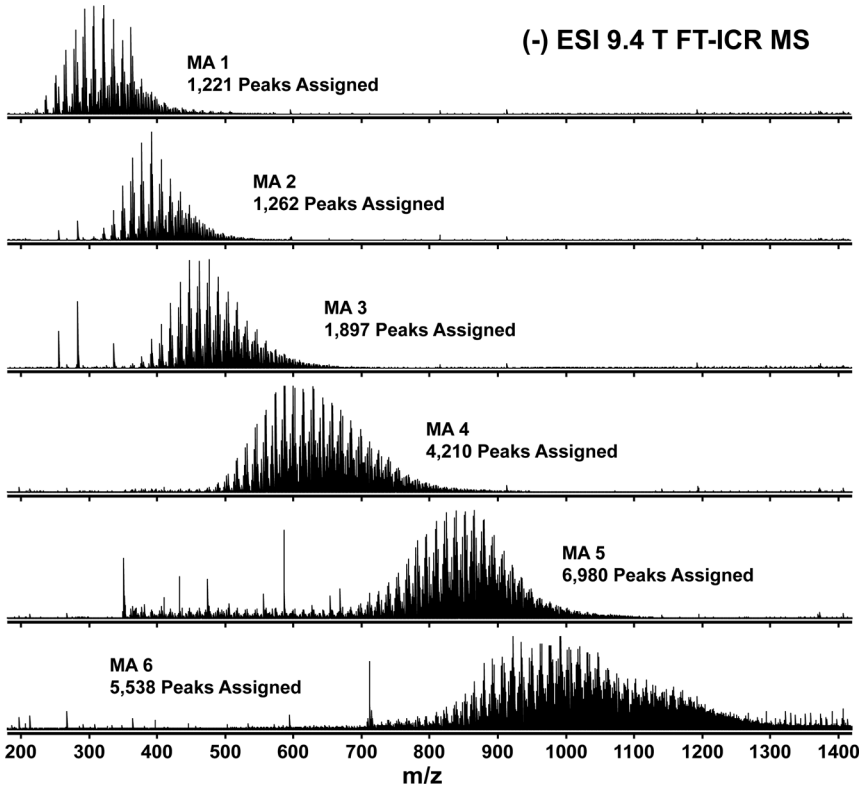

Figure 4. Negative ESI FT-ICR mass spectra for each of six MAPS extraction NAP acid fractions.

Mass Spectra Observed by MAPS Acid Isolation. Molecular weight fractionation reduces the complexity of each sample, thereby increasing dynamic range, and also separates easily ionized low-molecular-weight acids from the less efficiently ionized high-molecular-weight acids. Figure 4 shows the mass spectra for all fractions, MA 1−MA 6, of successively higher molecular weight, from MAPS extraction of Canadian bitumen NAP acids. Note the continuous distribution of NAP acids ranging from approximately 220 to 1450 Da. Because of acid fractionation by molecular weight, we are able to approximately double the observed mass range and approximately triple the number of unique elemental formulas assigned (from ∼4400 assignments by traditional characterization to ∼13 500 unique elemental assignments for MAPS fractions) for NAP acids from Canadian bitumen. The higher molecular weight NAP acids are present in the original mixture but are masked by the lower molecular weight NAP acids.

Heteroatom Class Composition. To better represent the mass spectral data, isoabundance-contoured plots of double bond equivalents (DBE) versus number of carbon atoms are constructed for the most abundant heteroatomic class compounds. Figures 5 and 6 represent the three most abundant heteroatom classes from MAPS fractionation. For the O_2 heteroatom class (Figure 5), the first fraction (MA 1) comprises the smallest, least hydrophobic NAP acids, predominately two and three cycloalkyl ring (DBE = 3 and 4) NAP acids containing ∼20 carbon atoms. Although the number of carbons increases for successive elution fractions, the most abundant DBE range stays approximately the same (DBE = 3−5), which is indicative of the typical NAP acid alicyclic structure.

For the O_2S_1 and O_2S_2 classes (Figure 6), DBE increases steadily for successive elution fractions. The early eluting

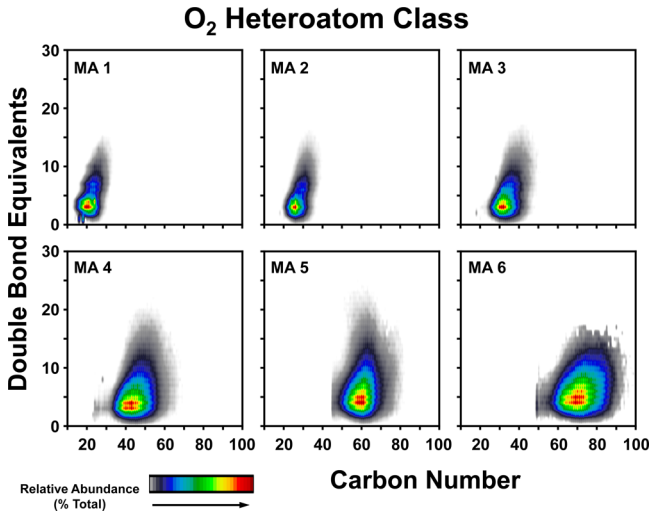

Figure 5. Negative ESI FT-ICR MS-derived isoabundance-contoured plots of DBE versus carbon number for the O_2 heteroatom class from MAPS acid extraction.

fractions (MA 1−MA 3) exhibit a slightly bimodal DBE distribution, indicative of a thiophenic carboxylic acid (DBE = 4−5) and thiophenic carboxylic acid with an additional aromatic ring (benzothiophenic, DBE = 7−8). In the final three fractions, low DBE compounds are not observed, and the most abundant species range from DBE 7 to DBE 14, likely corresponding to a mixture of additional fused cyclic and aromatic ring structures. The O_2S_2 heteroatom class extends to higher DBE than the O_2S_1 heteroatom class, presumably because of two thiophenic rings rather than one thiophenic ring.

dx.doi.org/10.1021/ef5015023 | Energy Fuels 2014, 28, 5043−5048

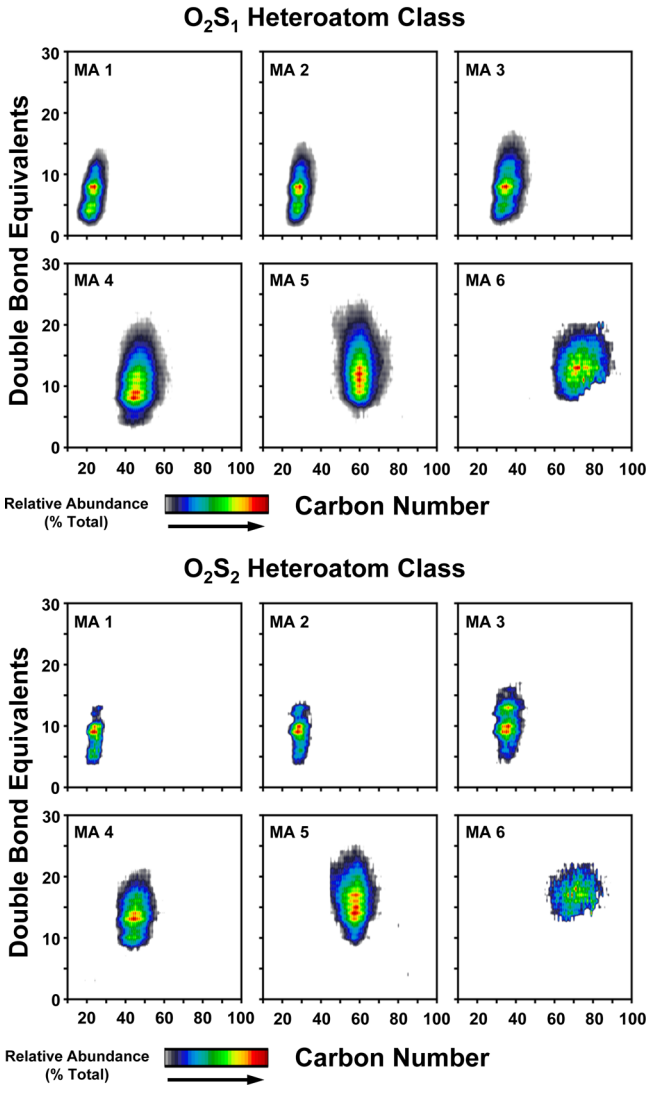

Figure 6. Negative ESI FT-ICR MS-derived isoabundance-contoured plots of DBE versus carbon number for the O_2S_1 and O_2S_2 heteroatom classes from MAPS acid extraction.

The isoabundance-contoured DBE versus carbon number plots for each fraction were overlaid into one plot for O_2, O_2S_1, and O_2S_2 classes and plotted along with the contour plots for the collectively isolated acids by the APS procedure in the top left of Figure 7. For the O_2 class, the DBE range at a low carbon number is limited. However, useful compositional data are extended from approximately 50 carbon atoms by collective isolation to approximately 90 carbon atoms by MAPS isolation (bottom left of Figure 7). Likewise, the observed carbon number range for O_2S_1 and O_2S_2 classes (top middle and top right of Figure 7) approximately doubles by MAPS isolation (bottom middle and bottom right of Figure 7). We also see a very different compositional pattern for sulfur-containing acids. The O_2 class adds predominately alkyl groups with increasing carbon number (low DBE values), whereas the O_2S_x compounds tend to add aromatic rings, as indicated by DBE spikes at three DBE intervals and a much larger increase in DBE with increasing the number of carbons.

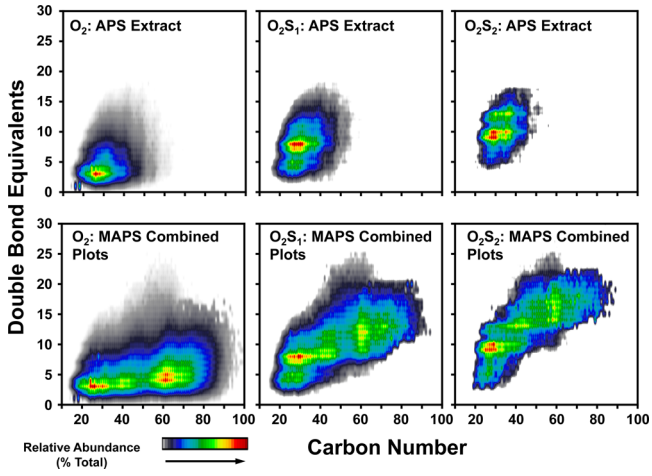

Figure 7. Negative ESI FT-ICR MS-derived isoabundance-contoured plots of DBE versus carbon number for APS and MAPS acid isolation. The top row of plots shows the collectively isolated and characterized plots for O_2, O_2S_1, and O_2S_2 heteroatom classes. The bottom row of plots is constructed from the combination of data from all MAPS acid mass spectra for the O_2, O_2S_1, and O_2S_2 heteroatom classes.

AUTHOR INFORMATION

Corresponding Author

*Telephone: +1-850-644-2398. Fax: +1-850-644-1366. E-mail: rodgers@magnet.fsu.edu.

Notes

The authors declare no competing financial interest.

ACKNOWLEDGMENTS

This work was supported by the National Science Foundation (NSF) DMR-11-57490, the Florida State University Future Fuels Institute, and the State of Florida. The authors thank Parviz Rahimi and the National Centre for Upgrading Technology for providing the distillation "broad cut" samples. The authors also thank Nathan K. Kaiser, John P. Quinn, and Greg T. Blakney for their continued assistance with instrumental maintenance and data analysis.

REFERENCES

(1) U.S. Energy Information Administration (EIA). *2012 World Proved Reserves*; EIA: Washington, D.C., 2013; http://www.eia.gov/countries/index.cfm?view=reserves#cabs (accessed March 3, 2014).
(2) Head, I. M.; Jones, D. M.; Larter, S. R. *Nature* **2003**, *426*, 344–352.
(3) Altgelt, K. H., Boduszynski, M. M. *Composition and Analysis of Heavy Petroleum Fractions*; Marcel Dekker, Inc.: New York, 1994.
(4) Headley, J. V.; Barrow, M. P. *Mass Spectrom. Rev.* **2009**, *28*, 121–134.
(5) Clemente, J. S.; Fedorak, P. M. *Chemosphere* **2005**, *60*, 585–600.
(6) Kilpatrick, P. K. *Energy Fuels* **2012**, *26*, 4017–4026.
(7) Baugh, T. D.; Grande, K. V.; Mediaas, H.; Vindstad, J. E.; Wolf, N. O. *Proceedings of the SPE 7th International Symposium on Oilfield Scale*; Aberdeen, U.K., May 11–12, 2005; SPE 93011.
(8) Mapolelo, M. M.; Stanford, L. A.; Rodgers, R. P.; Yen, A. T.; Debord, J. D.; Asomaning, S.; Marshall, A. G. *Energy Fuels* **2009**, *23*, 349–355.
(9) Kelland, M. A. *Production Chemicals for the Oil and Gas Industry*; CRC Press: Boca Raton, FL, 2009; pp 195–223.
(10) Freitas, S.; Malacarne, M. M.; Romão, W.; Dalmaschio, G. P.; Castro, E. V. R.; Celante, V. G.; Freitas, M. B. J. G. *Fuel* **2013**, *104*, 656–663.
(11) Slavcheva, E. *Br. Corros. J.* **1999**, *34*, 125–131.

(12) Jewell, D. M.; Weber, J. H.; Bunger, J. W.; Plancher, H.; Latham, D. R. *Anal. Chem.* **1972**, *44*, 1391−1395.
(13) Alfredson, T. V. *J. Chromatogr. A* **1981**, *218*, 715−728.
(14) Aske, N.; Kallevik, H.; Sjöblom, J. *Energy Fuels* **2001**, 1304−1312.
(15) Klein, G. C. G.; Angström, A.; Rodgers, R. P.; Marshall, A. G. A. *Energy Fuels* **2006**, *20*, 668−672.
(16) Shi, Q.; Hou, D.; Chung, K. H.; Xu, C.; Zhao, S.; Zhang, Y. *Energy Fuels* **2010**, *24*, 2545−2553.
(17) Barth, T.; Høiland, S.; Fotland, P.; Askvik, K. M.; Pedersen, B. S.; Borgund, A. E. *Org. Geochem.* **2004**, *35*, 1513−1525.
(18) Shepherd, A. G.; van Mispelaar, V.; Nowlin, J.; Genuit, W.; Grutters, M. *Energy Fuels* **2010**, *24*, 2300−2311.
(19) Colati, K. A. P.; Dalmaschio, G. P.; de Castro, E. V. R.; Gomes, A. O.; Vaz, B. G.; Romão, W. *Fuel* **2013**, *108*, 647−655.
(20) Juan, S. L.; Xian, S. B. *Pet. Sci. Technol.* **2009**, *27*, 1534−1544.
(21) Shi, L. J.; Shen, B. X.; Wang, G. Q. *Energy Fuels* **2008**, *22*, 4177−4181.
(22) Mediaas, H.; Grande, K. V.; Hustad, B. M.; Rasch, A.; Rueslåtten, H. G.; Vindstad, J. E. *Proceedings of the SPE 5th International Symposium on Oilfield Scale*; Aberdeen, U.K., Jan 29−30, 2003; SPE 80404.
(23) Qian, K.; Robbins, W. K.; Hughey, C. A.; Cooper, H. J.; Rodgers, R. P.; Marshall, A. G. *Energy Fuels* **2001**, *15*, 1505−1511.
(24) Smith, D. F.; Schaub, T. M.; Kim, S.; Rodgers, R. P.; Rahimi, P.; Teclemariam, A.; Marshall, A. G. *Energy Fuels* **2008**, *22*, 2372−2378.
(25) Jones, D. M.; Watson, J. S.; Meredith, W.; Chen, M.; Bennett, B. *Anal. Chem.* **2001**, *73*, 703−707.
(26) ASTM International. *Annual Book of ASTM Standards*; ASTM International: West Conshohocken, PA, 1999; pp 261−267.
(27) Parisotto, G.; Ferrão, M. F.; Müller, A. L. H.; Müller, E. I.; Santos, M. F. P.; Guimarães, R. C. L.; Dias, J. C. M.; Flores, E. M. M. *Energy Fuels* **2010**, *24*, 5474−5478.
(28) Yen, T.-W.; Marsh, W. P.; MacKinnon, M. D.; Fedorak, P. M. *J. Chromatogr. A* **2004**, *1033*, 83−90.
(29) Borgund, A. E.; Erstad, K.; Barth, T. *J. Chromatogr. A* **2007**, *1149*, 189−196.
(30) Marshall, A. G.; Blakney, G. T.; Chen, T.; Kaiser, N. K.; McKenna, A. M.; Rodgers, R. P.; Ruddy, B. M.; Xian, F. *Mass Spectrom.* **2013**, *2*, S0009−S0009.
(31) Hsu, C. S. *Energy Fuels* **2012**, *26*, 1169−1177.
(32) Rowland, S. J.; West, C. E.; Scarlett, A. G.; Jones, D. *Rapid Commun. Mass Spectrom.* **2011**, *25*, 1741−1751.
(33) McKenna, A. M.; Nelson, R. K.; Reddy, C. M.; Savory, J. J.; Kaiser, N. K.; Fitzsimmons, J. E.; Marshall, A. G.; Rodgers, R. P. *Environ. Sci. Technol.* **2013**, *47*, 7530−7539.
(34) Smith, B. E.; Sutton, P. a.; Lewis, C. A.; Dunsmore, B.; Fowler, G.; Krane, J.; Lutnaes, B. F.; Brandal, Ø.; Sjöblom, J.; Rowland, S. J. *J. Sep. Sci.* **2007**, *30*, 375−380.
(35) Mapolelo, M. M.; Rodgers, R. P.; Blakney, G. T.; Yen, A. T.; Asomaning, S.; Marshall, A. G. *Int. J. Mass Spectrom.* **2011**, *300*, 149−157.
(36) Hughey, C. A.; Rodgers, R. P.; Marshall, A. G.; Qian, K.; Robbins, W. K. *Org. Geochem.* **2002**, *33*, 743−759.
(37) Marshall, A. G.; Rodgers, R. P. *Acc. Chem. Res.* **2003**, *37*, 53−59.
(38) Rodgers, R. P.; Schaub, T. T. M.; Marshall, A. G. A. *Anal. Chem.* **2005**, *77*, 20A−27A.
(39) Hsu, C. S.; Hendrickson, C. L.; Rodgers, R. P.; McKenna, A. M.; Marshall, A. G. *J. Mass Spectrom.* **2011**, *46*, 337−343.
(40) Hindle, R.; Noestheden, M.; Peru, K.; Headley, J. *J. Chromatogr. A* **2013**, *1286*, 166−174.
(41) Kaiser, N. K.; Quinn, J. P.; Blakney, G. T.; Hendrickson, C. L.; Marshall, A. G. *J. Am. Soc. Mass Spectrom.* **2011**, *22*, 1343−1351.
(42) Blakney, G. T.; Hendrickson, C. L.; Marshall, A. G. *Int. J. Mass Spectrom.* **2011**, *306*, 246−252.
(43) Kelly, R. R. T.; Tolmachev, A. V. A.; Page, J. S.; Tang, K.; Smith, R. D. *Mass Spectrom. Rev.* **2010**, *29*, 294−312.
(44) Senko, M. W.; Hendrickson, C. L.; Emmett, M. R.; Shi, S. D. H.; Marshall, A. G. *J. Am. Soc. Mass Spectrom.* **1997**, *8*, 970−976.
(45) Kaiser, N. K.; Savory, J. J.; McKenna, A. M.; Quinn, J. P.; Hendrickson, C. L.; Marshall, A. G. *Anal. Chem.* **2011**, *83*, 6907−6910.
(46) Tolmachev, A. V.; Robinson, E. W.; Wu, S.; Kang, H.; Lourette, N. M.; Pasa-Tolić, L.; Smith, R. D. *J. Am. Soc. Mass Spectrom.* **2008**, *19*, 586−597.
(47) Savory, J. J.; Kaiser, N. K.; Mckenna, A. M.; Xian, F.; Blakney, G. T.; Rodgers, R. P.; Hendrickson, C. L.; Marshall, A. G. *Anal. Chem.* **2011**, *83*, 1732−1736.
(48) Ledford, E. B.; Rempel, D. L.; Gross, M. L. *Anal. Chem.* **1984**, *56*, 2744−2748.
(49) Shi, S. D.-H.; Drader, J. J.; Freitas, M. A.; Hendrickson, C. L.; Marshall, A. G. *Int. J. Mass Spectrom.* **2000**, *195−196*, 591−598.
(50) Xian, F.; Hendrickson, C. L.; Blakney, G. T.; Beu, S. C.; Marshall, A. G. *Anal. Chem.* **2010**, *82*, 8807−8812.
(51) Hughey, C. A.; Hendrickson, C. L.; Rodgers, R. P.; Marshall, A. G.; Qian, K. *Anal. Chem.* **2001**, *73*, 4676−4681.
(52) Corilo, Y. E. *PetroOrg Software*; Florida State University; All rights reserved. http://www.petroorg.com.
(53) Smith, D. F. D.; Rahimi, P.; Teclemariam, A.; Rodgers, R. P.; Marshall, A. G. *Energy Fuels* **2008**, *22*, 3118−3125.